CHAPTER 5

ELECTROCHEMICAL MODEL FOR CARBON-NANOTUBE ENFET (CNT- ENFET) WITH ZrO_2 AS DIELECTRIC FOR ACETYLCHOLINE DETECTION

CHAPTER 5

Electrochemical model for carbon-nanotube ENFET (CNT-ENFET) with ZrO_2 as dielectric for acetylcholine detection

5.1. An overview on CNT-ENFET

Intensive research on the traditional Si-based ENFETs has established a series of drawbacks such as scaling problem, low sensitivity, high threshold voltage, complex fabrication techniques and small on-off current ratio as discussed in Chapter 2. These drawbacks can be overcomed to a great extent with the use of CNT instead of Si material [20, 25, 50]. It is because semiconducting CNT exhibits properties including ballistic transport, biocompatibility, size compatibility, high chemical stability, robustness, good thermal and mechanical properties [4]. The easy synthesis of CNT in nano form reduces the scaling limitations of MOSFET. Because of these excellent properties, CNTFET based biosensors have received considerable attention for rapid testing of various analytes in various applications such as clinical diagnosis, biotechnology, medical applications, drug-delivery systems etc.

As far as integration of materials having high-κ dielectric into FET is concerned, a fundamental problem of conventional MOSFET devices is the degradation of its electrical properties due to carrier scattering mechanism introduced at the semiconductor- high-κ dielectric interface [47]. CNT has high compatibility with high-κ dielectric material imparted by their unique chemical bonding and surface stability. The electrostatic capacitance attainable with such gate insulators exceeds the quantum capacitance of CNTs, which is difficult to obtain by scaling SiO_2 films (low-κ dielectric) without producing large leakage currents. This capacitance enhances drain current and thus, on-off current ratio increases. Moreover, for the same capacitance, high-κ material requires small thickness compared to low-κ dielectric material [47, 49]. CNTs coated by high-κ dielectrics exhibit superior performance in subthreshold swings, high transconductance and mobility [49]. Thus, integration of high-κ material with CNT is a step forward towards device miniaturization.

As discussed in Chapter 2, acetylcholine is also a very important molecular carrier necessary for neurotransmission. It is an ester of choline and acetic acid serving as neurotransmitter in both central and peripheral nervous systems. Decrease in the levels of ACh in the body can cause many nervous system disorders like Alzheimer's disease, Schizophrenia, Huntington disease, Parkinson's disease and multiple sclerosis. Therefore, detection of acetylcholine is essential and significant. Thus, this chapter deals with the electrochemical modeling of chitosan/nickel oxide (CH/NiO) based carbon-nanotube ENFET (CNT- ENFET) with ZrO_2 as dielectric for acetylcholine detection.

The schematic of the fabricated CNT-ENFET has been shown in Fig. 5.1. It consists of ITO coated glass plate as substrate, ZnO as bottom insulator, K-doped carbon nanotube as n-type channel, drain and source regions, ZrO_2 as top gate insulator and chitosan/nickel oxide (CH/NiO) nanocomposite as sensing membrane arranged from bottom to top respectively. The structure of formation of CH/NiO composite with ZrO_2 and CNT has been shown in Fig. 5.2.

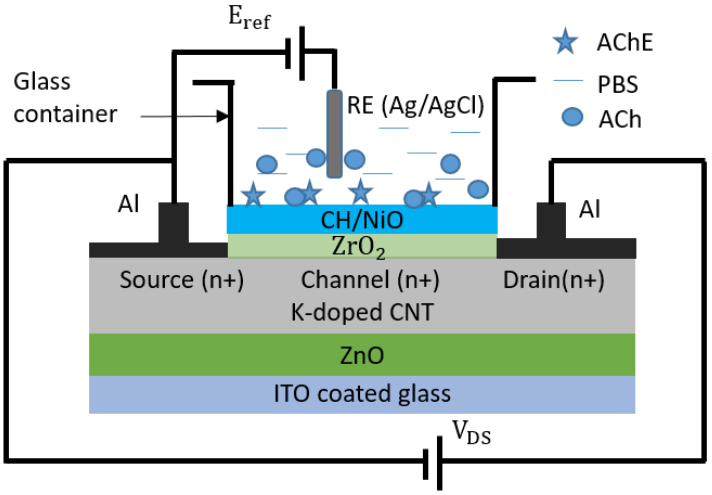

Fig. 5.1. Schematic of fabricated CNT- ENFET for Acetylcholine Detection

5.2. Fabrication and characterization of CNT-ENFET

The n-type CNTFET has been fabricated using chemical solution process. ITO coated glass has been used as substrate having dimension equal to 5 mm×2 mm. To minimize

the leakage current from channel to ITO, a thin insulating layer of intrinsic ZnO has been deposited on it. To deposit this layer, firstly ZnO solution is prepared as: 10 mg zinc acetate (Zn $(CH_3COO)_2$) has been dissolved in 10 ml distilled water. To this mixture, 2 ml ammonium hydroxide (NH_4OH) has been added and stirred at room temperature for about 30 minutes. Then, the solution is used for deposition using the ECD technique by applying a voltage of 4 to 5 V for about 20 to 25 minutes. After deposition, it is dried under room temperature. The thickness of ZnO layer has been measured by using the gravimetric analysis technique as discussed in Chapter 2. The desired thickness for ZnO layer is 10 nm. The process of deposition is continued until the desired thickness is obtained.

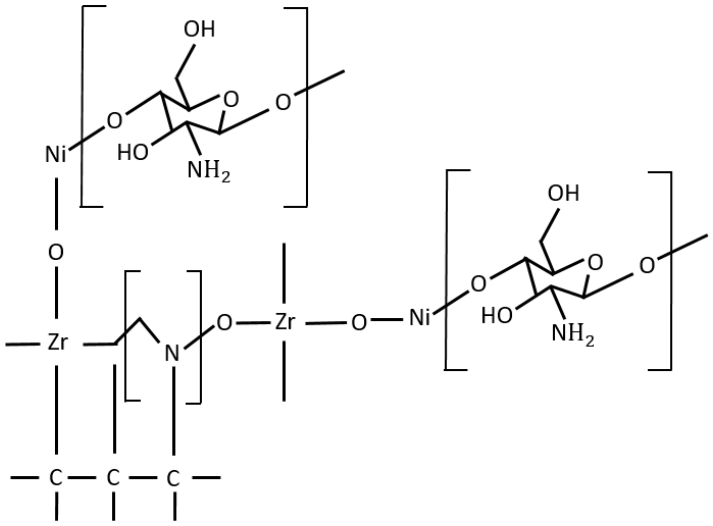

Fig. 5.2. Structure of formation of CH/NiO composite with ZrO_2 and CNT

On top of this ZnO layer, K-doped (doping concentration~10%) multiwall carbon nanotube (MWCNT) which acts as n-type source (S), drain (D) and channel regions (dimension is equal to 5 mm×2 mm×100 nm) has been deposited. To make CNT layer, firstly CNT solution has been prepared as: 10 mg CNT has been dispersed in 10 ml methanol and sonicated for about 2 hours [61, 90]. Boiling acid treatment technique has been used for its functionalization before use [26]. Since, potassium is very reactive with water and oxidizes rapidly in air, therefore, to dope CNT with K, at first solid KOH has been dissolved in pure water using magnetic stirrer to form a solution. KOH solution forms K^+ ions, OH^- ions and releases heat. These K^+ ions attach to carbon atoms making CNT an n-type material. Doping with K increases electrical conductivity

of CNT [50]. This doped CNT solution is used in the three-electrode system for deposition. A voltage of 2 to 3 V is applied between the WE and CE and kept for about 20 to 30 minutes. The thickness is measured using gravimetric analysis technique. Then, it is dried under room temperature.

On top of the channel region of CNT, a thin layer of ZrO_2 having dimension equal to 1 mm×2 mm×10 nm is deposited. ZrO_2, which being a high-κ dielectric (κ~25) increases capacitance and reduces direct tunneling leakage current [47, 49, 97]. This increased capacitance enhances device performance. In addition, it is highly compatible with CNTs leading to device miniaturization. For deposition of this layer, at first 100 mg solid ZrO_2 is dissolved in 10 ml water and sonicated for 15 to 25 minutes. This layer is deposited only on the channel region, so, the area for source and drain contact is masked using Teflon tape [29] while the deposition is done using ECD technique by applying a voltage of 4 to 5 V for about 20 to 25 minutes. The thickness is measured using gravimetric analysis technique. After deposition of ZrO_2 film, it is dried by heating it at 180 ºC. Then, NiO/CH nanocomposite has been deposited on the gate insulator (dimension is equal to 1 mm×2 mm×50 nm) as sensing membrane because it is a very attractive material for biosensor applications due to its excellent film forming ability, mechanical strength and biocompatibility [9]. NiO film is prepared by using the method of solution. Here, 20 ml each of NaOH and $NiCl_2.6H_2O$ of 100 mM concentration is dissolved in 20 ml distilled water at room temperature and deposited using ECD technique by applying 4 to 5 V. The area for source and drain contact is masked using Teflon tape. This layer is then heated at 290 ºC to get a thin film of solid nano-NiO [98]. To improve the biocompatibility of NiO, it is doped with 10 µl of CH. For this, 0.05 M CH solution is prepared by adding 50 mg in 100 ml of acetate buffer. This CH solution is uniformly spread over the nano-NiO film and dried at room temperature for about 24 hours to get the NiO/CH nanocomposite layer. Then, the Teflon tape is removed and the device is washed with de-ionized water to remove any unbound particles.

Aluminum (Al) metal has been used as contact for source and drain regions because it has low melting point, low resistivity, excellent adhesion to dielectrics, ease of deposition and no contamination. It is deposited using filament evaporation technique. The contact between Al and CNT is quasi-ohmic because Al has work function less

than CNT. So, to make ohmic contact, CNT is heavily doped with K, which raises the Fermi level closer to the conduction band, thereby matching its Fermi level with that of Al. This is known as depinning technique as discussed in Chapter 2.

Referring to experimental part, experiments need to be performed to see the gate dependence similarity of the device both outside (CNT-MOSFET) and in-liquid (CNT-ENFET) measurements.

For the measurements outside the liquid: aluminum metal (work function 4.08 eV) has been deposited on the top of the ZrO_2 layer (by filament evaporation technique) that acts as the gate of MOSFET. Experiments have been performed to find the output and transfer characteristics of the device outside the liquid. For output characteristic curves, d.c. drain currents measured by digital multimeter (DMM) have been plotted against drain voltages from 0 to 1 V, in step of 0.1 V with some applied gate voltages from 0.2 to 0.5 V, in step of 0.1 V as shown in Fig. 5.3. Similarly, the transfer characteristic curve has been drawn (for V_{DS} = 0.4 V) as shown in Fig. 5.4. The threshold voltage from the transfer characteristic curve has been obtained by using extrapolation in linear region method (ELR) and found as ~ 0.1V. In this technique, the tangent is drawn at the linear region giving the maximum slope.

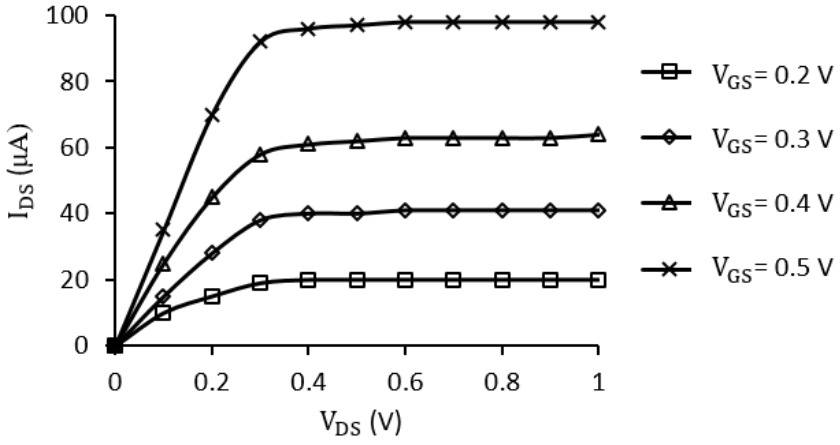

Fig. 5.3. Output characteristics of CNT-MOSFET

For in liquid measurements (CNT-ENFET): 1 M AChE solution has been prepared by dissolving 1mg of AChE powder in 1 ml Phosphate Buffer Saline (PBS, 50 mM and

pH 7) and stored at 4º C. 0.2 mM ACh solution has been prepared in pure water. As liquid measurement occurs in this device, so, passivation of the whole device except the sensing area is necessary. For this polydimethylsiloxane (PDMS) coating is done [105]. Once the fabrication of the device is complete, 1 µL of enzyme AChE is immobilized on the sensing membrane by using physical adsorption technique [88]. Then, the device is dried overnight and stored in refrigerator at 4 ºC, when not in use.

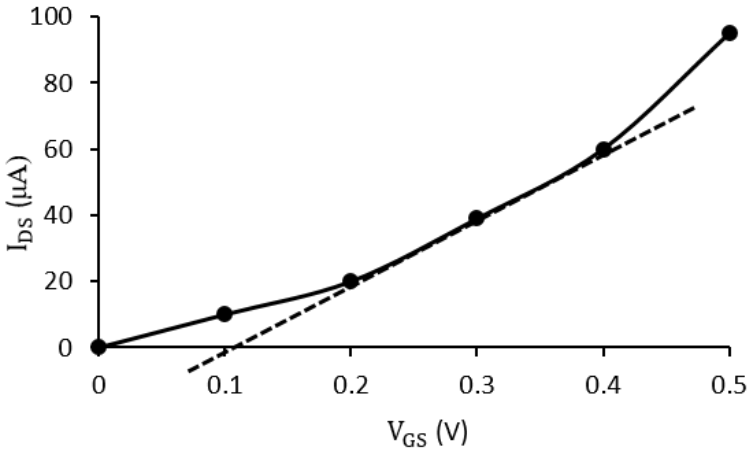

Fig. 5.4. Transfer characteristics of CNT-MOSFET to extract $V_{TH,CNT-ENFET}$ using ELR technique

Firstly, to get the output characteristics, ACh concentration is varied from 0.01 to 0.2 mM and corresponding I_{DS} is recorded by varying V_{DS} from 0 to 0.6 V. The results have been plotted in Fig. 5.5. To get the transfer characteristics, different ACh solution is taken and its pH is measured. For these solutions having different pH, I_{DS} current has been recorded with varying V_{GS}. Fig. 5.6 shows V_{GS} vs I_{DS} plot for ACh solution having pH 7, 6.5 and 5.75 for V_{DS} = 0.2 V.

5.3. CNT-ENFET MODEL

An electrochemical model of the fabricated device has been developed. The modeling has been done considering each layer of the device. The different layers of the device

along diffusion length (x) is shown in Fig. 5.7. The modeling and simulation results have been discussed in details in the following subsections.

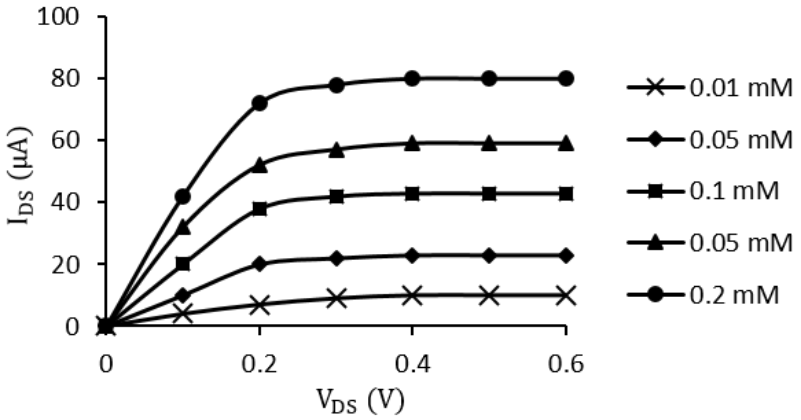

Fig. 5.5. Output characteristics of CNT-ENFET

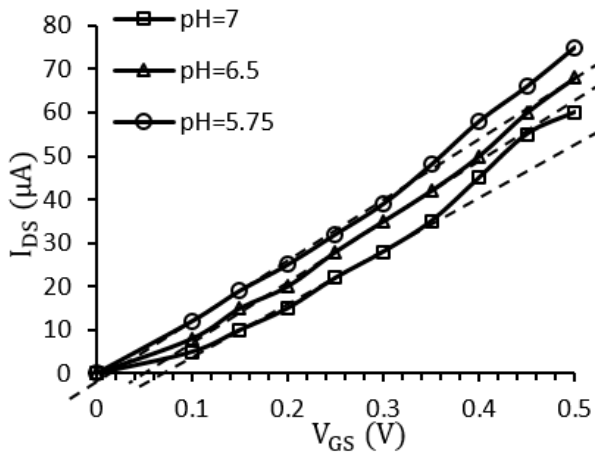

Fig. 5.6. Transfer characteristics of CNT-ENFET

5.3.1. Modeling of acetylcholinesterase enzymatic reactions

From the experiments performed, it is evident that bio-chemical reaction takes place in the enzyme layer. Therefore, the conventional enzyme kinetics can be used for modeling the enzymatic layer. The AChE enzyme catalyzes the hydrolysis of ACh in acetic acid and choline as shown in Eq. (5.1).

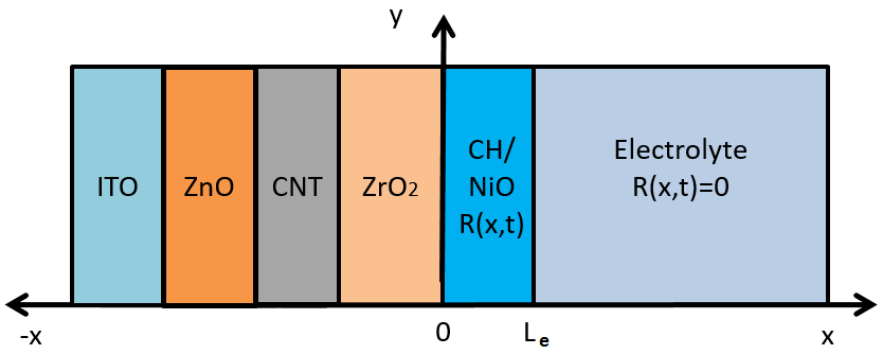

Fig. 5.7. Description of CNT-ENFET structure with respect to diffusion length (x)

$$Acetylcholine + H_2O \xrightarrow{\substack{Acetylcholine \\ esterase}} Acetic\ acid + Choline \qquad (5.1)$$

Choline is an ammonium salt, which is soluble in water and does not participate in pH detection. Acetic acid is the primary product for pH change to occur. The enzymatic reaction has been modeled by using Michaelis –Menten equation as shown by Eq. (3.8) of Chapter 3.

5.3.2. Modeling of diffusion of acetylcholine and acetic acid in PBS solution

The modeling has been done using the diffusion model discussed in Chapter 3 taking $[S]$ = ACh concentration and $[P]$ = acetic acid concentration. Fig. 5.8 shows the $[S]$ and $[P]$ variations in the enzyme layer with x. The diffusion of substrate molecules occurs from the bulk electrolyte into the enzyme layer. Therefore, it is noticed from the graph that from L_e to 0, $[S]$ decreases and $[P]$ increases following the Fick's law of diffusion. Beyond the enzyme layer, i.e. when $x > L_e$ in the bulk electrolyte $[S]$ is constant and $[P]$ is almost zero.

5.3.3. Modeling pH variations due to release of H^+ ions

The product, CH_3COOH releases H^+ ions in the presence of water, which contribute towards the change in pH at the enzyme- insulator interface (Eq. (5.2)).

$$CH_3COOH \xrightarrow{H_2O} CH_3COO^- + H^+ \tag{5.2}$$

The acid dissociation constant (K_a) of acetic acid obtained from Eq. (5.2) is given by Eq. (5.3). Charge neutrality concept is used in Eq. (5.4). The initial H^+ ion concentration (C_i) determined by the pH of the buffer solution (pH_0) and K_e as given by Eq. (3.41) of Chapter 3.

$$K_a = \frac{[CH_3COO^-][H^+]}{[CH_3COOH]} \tag{5.3}$$

$$[H^+] = [CH_3COO^-] + [OH^-] + C_i \tag{5.4}$$

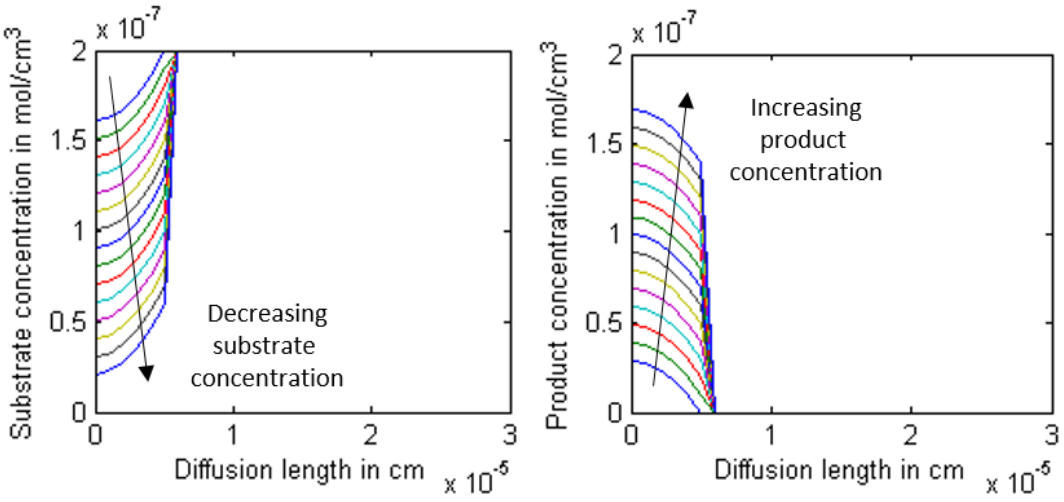

Fig. 5.8. Substrate and product concentration variation with diffusion length at different time

Now, using the above equations, we get,

$$[H^+]^2 - C_i.[H^+] - K_a.[P](x,t) - K_e = 0 \tag{5.5}$$

Solving the Eq. (5.5), we get the H^+ ion concentration and using the result, we get the pH changes at the ISFET's surface. With increase in $[P]$, H^+ ion concentration also increases which signifies that the solution near the surface of the ISFET is getting more acidic with a decrease in pH value.

Fig. 5.9 shows the variation of pH with the diffusion length with increase in [P]. A decrease in pH is observed moving closer towards the ISFET's surface, as the enzymatic reactions are more prominent at the enzyme insulator interface. When the H^+ ion concentration becomes much higher in the enzyme layer then the pH becomes almost constant throughout the layer.

5.3.4. Current transport model for CNT-ENFET

The change in pH results in $\psi_{0,CNT-ENFET}$ variation as given by Bousse's model in Eq. (2.13) of Chapter 2. $\psi_{0,CNT-ENFET}$ increases with a decrease in pH as shown in Fig. 5.10A. The modeling results have also been compared with the experimental results of $\psi_{0,CNT-ENFET}$ showing a good fit. This experimental curve has been obtained by using the experimentally obtained threshold voltages from the transfer characteristic curves using ELR method at different pH values of ACh solution as shown in Fig. 5.6 and then using the Eq. (4.11) of Chapter 4. The sensitivity parameter β has been found to be 62.2 considering number of surface sites (N_S) to be 10 x 10^{14} cm^{-2} and (C_{eq}) to be 20 µFcm^{-2} [22]. From modeling results, the sensitivity has been found to be 58.2 mV/pH, which is comparable to experimentally determined sensitivity i.e. 58 mV/pH. The sensitivity of the ZrO_2 insulating material is high, so, small variations in pH resulted in considerable potential variations, which can be detected by the device.

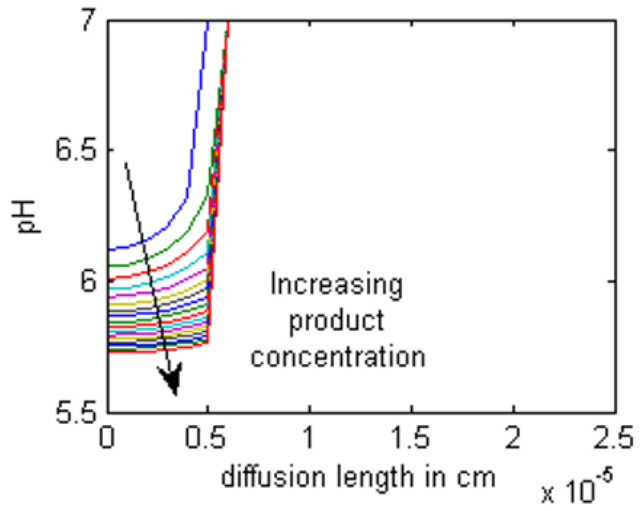

Fig. 5.9. Diffusion length vs pH with increasing product concentration

Referring to the modeling of ENFET threshold voltage, the changes in $V_{TH,CNT-ENFET}$ with pH can be obtained using Eq. (5.6).

$$V_{TH,CNT-ENFET} = E_{ref} - \psi_0 + \chi_{sol} - \frac{\Phi_{CNT}}{q} - \frac{Q_{ox} + Q_{ss} + Q_{CNT}}{C_{ox}} \tag{5.6}$$

where, Φ_{CNT} is the work function of CNT and Q_{CNT} is the charge present in CNT. In the threshold voltage calculation for Si or other MOSFET's, a $2\Phi_f$ (Φ_f is the Fermi potential of the bulk semiconductor) term is also present which gives the inversion potential. But for CNTFET, this term is not included because no inversion occurs as CNT channel is already present.

The charge present in CNT i.e. Q_{CNT} can be determined using the expression as given in Eq. (5.7) [82].

$$Q_{CNT} = -qn_{CNT}L_{CNT} \tag{5.7}$$

where, n_{CNT} is the number of charge carriers present in the CNT and L_{CNT} is the length of the CNT.

The threshold voltage varies from about 0.02 V to 0.08 V with increasing pH as shown in Fig. 5.10B. It also shows good agreement between the modeling and experimental values of threshold voltage. The experimental threshold voltage with respect to pH has been obtained by using ELR method in the experimentally obtained transfer characteristic curves shown in Fig. 5.6.

It is clear from Fig. 5.5 that the fabricated CNT-ENFET behaves like a MOSFET. The current transport equations for ENFET shown in Eqs. (3.45) and (3.46) of Chapter 3 can, therefore, be used by replacing $V_{TH,ENFET}$ with $V_{TH,CNT-ENFET}$. Fig. 5.11 shows a comparison between the simulation and experimental results in terms of output drain current with drain to source voltage. A good fit is seen between the two plots. Values of various parameters which have been found much influential during simulation are tabulated in Table 5.1.

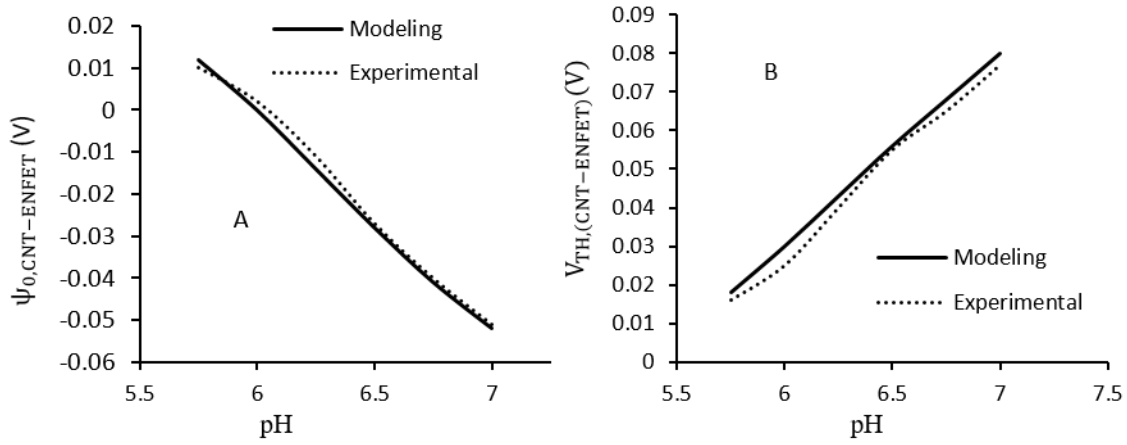

Fig. 5.10. (A) pH vs $\psi_{0,CNT-ENFET}$ plot showing comparison between modeling and experimental data. (B) pH vs $V_{TH,CNT-ENFET}$ plot showing comparison between modeling and experimental data

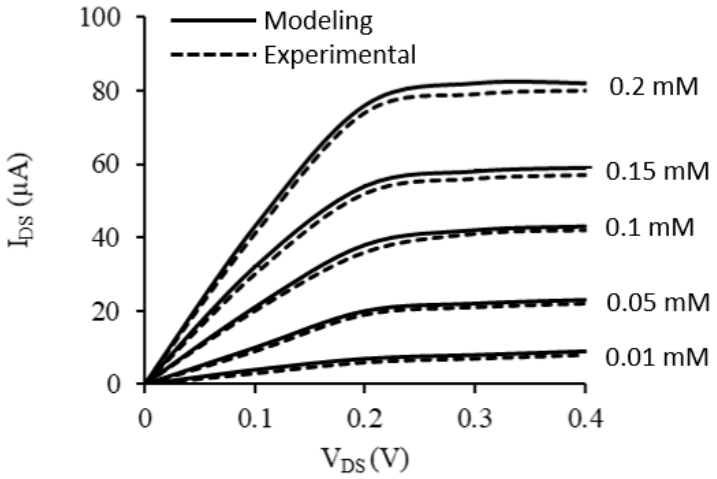

Fig. 5.11. Output characteristics of CNT-ENFET showing comparison between modeling and experimental results

5.4. Summary

In this work, an electrochemical model for CNT based ENFET has been developed and simulated considering the enzymatic reactions, diffusion phenomena, acid/base reactions, pH detection properties of ISFET and current transport model of CNTFET. The model has been successfully validated with the fabricated device characteristics for

acetylcholine detection showing good agreement with the experimental results. From modeling and simulation results, it may be concluded that even if a transition takes place from Si domain to CNT domain, the basic theory and principle associated with conventional Si based ENFET devices will also be applicable to CNT-ENFET devices.

Table 5.1: Values of various parameters considered for CNT-ENFET modeling

Sl. No.	**Parameter**	**Values**
1.	Maximal enzyme activity (a_M)	16.67×10^{-9} mol/s for 1 AChE unit
2.	Number of enzymatic units per volume (n_{enz})	301×10^{4} AChE units/cm^3
3.	Michaelis Menten Constant (K_M)	0.2 mM
4.	Acetylcholine diffusion constant (D_S)	8×10^{-6} cm^2/s
5.	Acetic acid diffusion constant (D_P)	1.08×10^{-5} cm^2/s
6.	Enzyme layer thickness (L_e)	50 nm
7.	Acid dissociation constant for acetic acid (K_a)	1.75×10^{-5}
8.	Reference Voltage (E_{ref})	0.6 V
9.	pH of PBS solution (pH_0)	7
10.	Surface dipole potential of the solvent (χ_{sol})	0.3 V
11.	Number of charge carriers present in CNT (n_{CNT})	6×10^{15} cm^{-3}
12.	Length of CNT (L_{CNT})	5 mm
13.	Average work function of CNT (ϕ_{CNT})	4.7 eV
14.	Thickness of ZrO_2 layer (t_{ox})	10 nm
15.	Electron mobility of CNT (μ)	10000 cm^2/Vs
16.	Width of channel (W)	2 mm
17.	Length of channel (L)	1 mm